J Mater Sci (2006) 41:8059–8067
DOI 10.1007/s10853-006-0417-9

An impedance study of the electrophoretic deposition from yttrium silicate suspensions

Chr. Argirusis · T. Damjanović · O. Schneider

Received: 21 December 2005 / Accepted: 8 May 2006 / Published online: 28 October 2006

Abstract Yttrium silicate powders were prepared according to a modified Pechini method. The powders were dispersed in isopropanol and the conditions of electrophoretic deposition from these suspensions were optimized. Well adhering coatings were obtained. Impedance spectroscopy was applied to characterize the solvent and the suspension as well as to study the causes for the rapid current decay recorded during constant voltage deposition. Specific conductivity and dielectric constants of solvent and suspension were extracted as well as the resistance of the deposit. Results indicate that mainly mass transport processes through the deposited layer are responsible for the current decay, and to a much lesser extent the resistance of the deposit.

Introduction

Yttrium silicates (YSI) seem to be one of the best candidates for a coating material for carbon–carbon composites because of their excellent properties such as a thermal expansion coefficient similar to that of SiC, a low evaporation rate and low oxygen permeation [1].

In our previous works we used electrophoretic deposition (EPD) to produce mullite layers for extended oxidation protection of C/C–Si–SiC composites [2–6] as well as electrodes and electrolytes for solid oxide fuel cells [7, 8].

The aim of this work was to prepare yttrium silicate suspensions by synthesizing and dispersing a powder in organic solvent and test their suitability regarding electrophoretic deposition.

In the literature it was repeatedly reported that during constant voltage EPD the current and therefore the deposition rate decrease with time [9]. The same had been observed in earlier studies of some of the authors of the present paper [5, 7]. Several factors have been claimed to contribute to this behavior: depletion of particles due to deposition [10, 11], a large resistance of the deposit formed [9], and mass transport limitations through the growing deposit layer [12]. In order to clarify the relevance of these factors for the EPD of YSI, we decided to characterize solvent, suspensions and YSI deposits via impedance spectroscopy. In addition, the current transients during EPD were to be recorded and compared with the impedance data.

Powder preparation

The YSI powders were prepared by a modified Pechini method, which allows the preparation of fine and homogeneous powders. The sol–gel method can also be used to produce yttrium silicate powders but it is experimentally more complicated as compared to the combustion method [13]. The Pechini method is a

Chr.Argirusis (✉) · T. Damjanović · O. Schneider
Institut für Metallurgie, Technische Universität Clausthal, Robert-Koch-str. 42, Clausthal-Zellerfeld D-38678, Germany
e-mail: christos.argirusis@tu-clausthal.de

T. Damjanović
e-mail: tanja.damjanovic@tu-clausthal.de

O. Schneider
e-mail: oliver.schneider@tu-clausthal.de

precursor based method of synthesis. For our purpose we used an aqueous solution of ethyleneglycole, citric acid and yttrium nitrate ($Y(NO_3)_3 * 6H_2O$) as a source of yttrium, with addition of TEOS or SiO_2 powder (Aerosil200, Degussa GmbH, Germany) as a source of silicon. This mixture was first heated on a hot-plate till the vapors of nitrogen oxides disappeared, and then sintered in a furnace in air. After this procedure we already obtained crystalline powders at 1100 °C.

The produced powders (Y_2SiO_5 and $Y_2Si_2O_7$) were further used separately or as a mixture (70 wt% $Y_2Si_2O_7$ and 30 wt% Y_2SiO_5) [14] for the production of dispersions in isopropanol suitable for electrophoretic deposition. The suspension for this study was prepared by dispersing an Y_2SiO_5 powder with iodine in isopropanol in ultrasonic bath for 15 min [7, 15]. The resulting suspension was kept on magnetic stirrer before use. The concentration used was 10 g/l. The suspension volume used in the experiments usually was 200 ml.

Description of impedance spectroscopy

Impedance spectroscopy is a standard technique in electrochemistry [16, 17], but has been rarely applied in the field of EPD [18]. In the three-electrode configuration, an alternating voltage is applied between a working electrode (WE) and a reference electrode (RE), and the current flowing between WE and a counter electrode (CE) is measured. From the ratio of voltage and current, the impedance (Z) between WE and RE can be calculated. This configuration has the advantage that only electrode processes at the WE contribute to the impedance. In the two electrode configuration, the CE is used as RE at the same time, and reactions at both electrodes and the medium (e.g., the solution) can contribute to the impedance. By varying the applied frequency (f) over several decades (MHz–mHz), informations about material conductivities, dielectric constants, electrochemical reaction rates, interfacial capacitances, mass transport processes and others can be obtained. The shape of the spectra can inform about the physical processes taking place in the system under study. A common representation is to plot the imaginary part of the complex impedance ($\mathrm{Im}(Z)$) versus its real part ($\mathrm{Re}(Z)$) in the complex plane (Nyquist plot). In order to analyze the data quantitatively it is necessary to make a physical model of the system and fit the data with this model. Very often the model is written in the form of an electrical equivalent circuit (EC), using standard circuit elements like capacitors, resistances, and inductances, but also special elements, like the constant phase element reflecting a non-ideal (frequency-dependent) capacitance, or the Warburg impedance, that describes diffusion processes. This approach was applied in the present paper.

Experimental setup

All measurements were performed using a home-built EPD setup, which allows to control the electrode distances with a micrometer screw. For impedance measurements of the properties of isopropanol and YSI suspensions, two glass slides were sputter-coated with gold on one side. The total area covered with gold was 9.97 cm^2. The area exposed to solution during the experiments was 5.2 cm^2. The actual YSI-deposition experiments were carried out using a glassy carbon (GC) substrate ($20 \times 20 \times 2$ mm^3) as working electrode and two gold-coated glass slides as counter electrodes. The gold-coated sides of the slides each faced one side of the GC substrate, at a constant distance. Deposition was performed by applying a voltage supplied by a Statron power supply (0–150 V, 0–4 A) between substrate and the counter electrodes, the GC substrate being the negative pole. Current transients were recorded using a Hameg HM 8112-2 multimeter equipped with a HAMEG-multiplexer. The suspensions were stirred during deposition with a magnetic stirrer. Impedance measurements were carried out in the two electrode configuration (with the Statron power supply disconnected). The frequency was varied between 500 kHz and 1 Hz, except if noted otherwise. For the measurements in pure solvent and suspension without deposition, one of the Au electrodes was connected to the working electrode (WE) input of the impedance setup (Zahner elektrik IM6), and the other one to counter (CE) and reference electrode (RE) inputs. For the EPD experiments, a GC substrate was connected to the WE input, and both gold electrodes (shortened) to CE and RE inputs.

Results

Impedance characterization of isopropanol and the suspension

Both isopropanol and the suspension for EPD were characterized by impedance measurements with the Au-coated glass slides as electrodes. Spectra were measured at different electrode distances in order to extract the specific conductivity and the dielectric

constant of solvent and suspension. The impedance data for pure isopropanol were characterized by a single semicircle in the complex plane. At high frequencies all spectra passed through the origin ($\mathrm{Re}(Z) = 0\ \Omega$). The low frequency intercept R_{LF} with the $\mathrm{Re}(Z)$ axis increased with increasing electrode distance. Figure 1 shows a plot of R_{LF} (circles) as a function of the electrode distance along with a linear fit. R_{LF} increases linearly with the electrode distance. This shows that the ohmic resistance of the isopropanol between the gold electrodes controls the width of the semicircle. However, the fit line does not pass through the origin, but shows an intercept of 16.4 MΩ cm^2. Therefore the data were fitted to the equivalent circuit shown in Fig. 2. C represents the capacitance of the isopropanol solution between the Au electrodes, R_{sol} the ohmic resistance of the isopropanol, R_{if} an interfacial resistance and CPE an interfacial capacitance, described by a constant phase element. The spectra were fitted to this equivalent circuit, keeping the value for R_{if} fixed at 16.4 MΩ cm^2. The fit results for R_{sol} (squares) are shown as well in Fig. 1, along with a linear fit of the data through the origin. From the slope of the plot, which equals the specific resistivity of the isopropanol, one obtains a value of $1.0 \times 10^{-7} \pm 2 \times 10^{-9}$ S cm^{-1} for the specific conductivity.

The dielectric constant of the isopropanol solution was derived from the slope of a plot of the capacitance versus the reciprocal electrode distance. Considering the contribution of the part of the electrode in air above the isopropanol, a dielectric constant of $\varepsilon_r = 25.6 \pm 3.7$ was obtained.

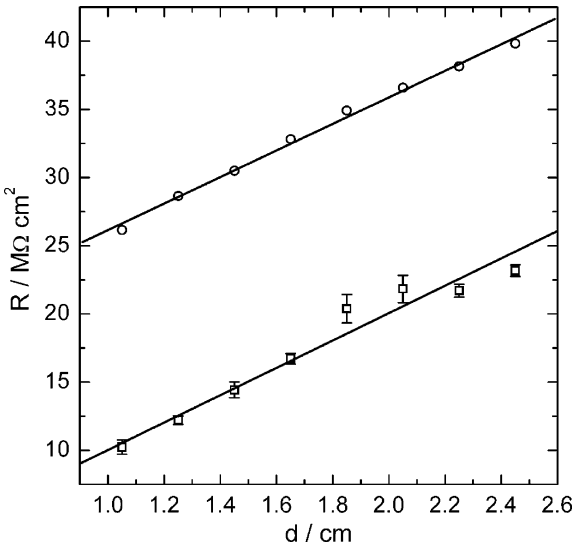

Fig. 1 Characteristic resistances obtained from IS measurements between two gold coated glass slides immersed in pure isopropanol. Circles: Low frequency intercept of semicircle in the complex plane. Squares: Fit results for R_{sol} after fitting to the equivalent circuit shown in Fig. 2. Lines: Linear fits of the data

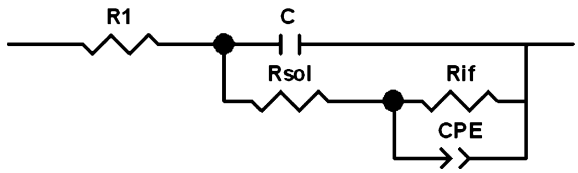

Fig. 2 Equivalent circuit for the analysis of impedance data in isopropanol. $R1$: cable resistance, C: capacitance, R_{sol}: resistance of solvent, R_{if}: interfacial resistance, CPE: constant phase element describing capacitance of the interface

Impedance spectra for the YSI suspension are presented in Fig. 3. They are characterized by a partial high frequency semicircle, the diameter of which again increases with increasing electrode distance. The resistance values are much lower than for the pure isopropanol, which explains why the maximum of the semicircle was not seen in the measurements. A simple parallel combination of a resistor and a capacitor was sufficient to describe the data. The process at low frequencies, where real and imaginary part of the impedance increased again, was not considered for the analysis. Analysis like before resulted in a specific conductivity of the suspension of $1.02 \times 10^{-4} \pm 1 \times 10^{-6}$ S cm^{-1}, and a dielectric constant of $\varepsilon_r = 31.7 \pm 2.9$.

Electrophoretic deposition of YSI: current transients and impedance data

YSI was deposited stepwise onto GC substrates in order to study the influence of a deposit on the

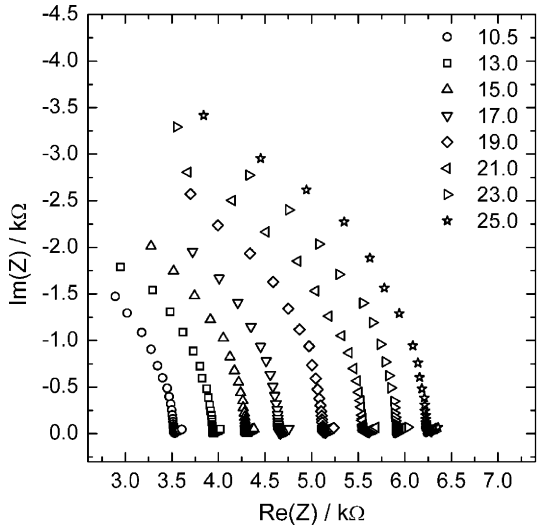

Fig. 3 Impedance spectra measured between two gold coated glass slides immersed in YSI suspensions at various electrode distances. Electrode area: 5.2 cm^2. Electrode distances in the legend are given in mm

electrodes and especially of its resistance on the further deposition process. For each deposition step, a voltage of 100 V was applied for a duration of 60 s. Thereafter the voltage was turned off, and two impedance spectra were recorded at open circuit (about 0 V), followed immediately by the next deposition step. The cumulative deposition time was 6–7 min. The experiment was repeated with several substrates. The deposited films adhered well to the substrates.

Typical current transients are shown in Fig. 4. A rapid decay of the current was observed in each deposition step. The currents at the end of each deposition step decreased from step to step. The current at the beginning of a new deposition step was always much larger than the current in the end of the preceding step, but much smaller than in the beginning of the experiment when no deposit was present on the electrode, and also showed a tendency to decrease. The insert in Fig. 4 shows another transient recorded during continuous EPD of YSI on GC at 75 V for 10 min showing the typical current decay during constant voltage EPD. Figure 5 shows the corresponding (cumulative) charge–time curve that was obtained by integration of the current data. The entire charge measured during the first deposition step was as large as the total charge of the remaining five steps. The general shape of the charge–time curve was similar to the one obtained for continuous deposition (insert in Fig. 5). In the latter case, the total charge was 1.7 C. The mass of the deposit after drying the GC substrate (total electrode area: 9.6 cm^2) in air was 86.7 mg. Normalization to the charge gives 51 mg/C.

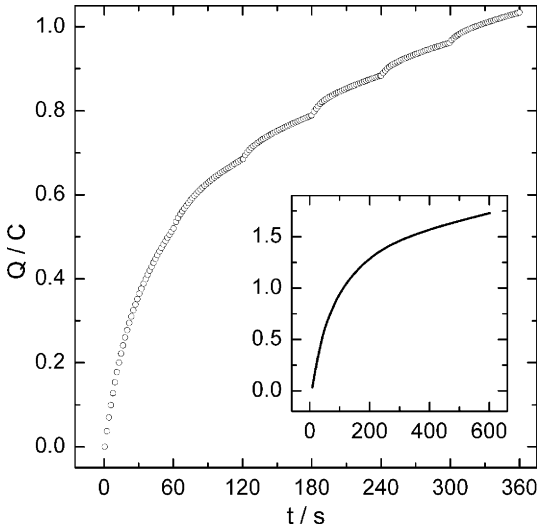

Fig. 5 Charge flux (obtained from integration of data shown in Fig. 7) during stepwise YSI deposition onto glassy carbon (100 V, 60 s, 6–7 repeats). Insert: Charge flux during continuous YSI deposition onto glassy carbon (75 V, 10 min)

The shape of the impedance spectra was similar to those shown in Fig. 3. All spectra showed a partial high frequency semicircle, and a second, smaller semicircle at lower frequencies (~<1 kHz). There was a difference between the first and second IS measurement after each deposition step. This is shown exemplarily in Fig. 6. The spectra measured immediately after turning off the deposition voltage showed higher resistances for both semicircles. In addition the data quality often was not as good as in the second spectrum, and even inductive loops between the two semicircles could be

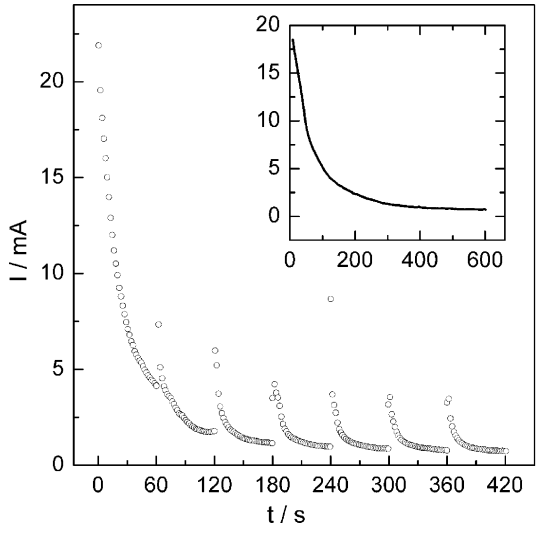

Fig. 4 Current transients recorded during stepwise YSI deposition onto glassy carbon (100 V, 60 s, 6–7 repeats). Insert: Transient recorded during continuous YSI deposition onto glassy carbon (75 V, 10 min)

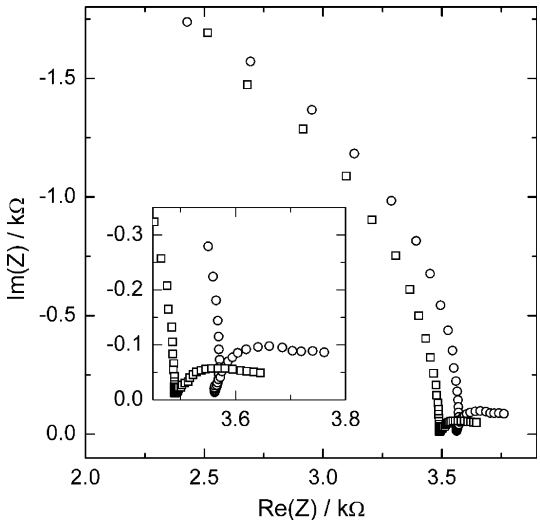

Fig. 6 First (circles) and second (squares) IS spectra measured after the 5th electrophoretic deposition step of YSI on GC. Total deposition time: 300 s. In the insert the low frequency region is shown enlarged

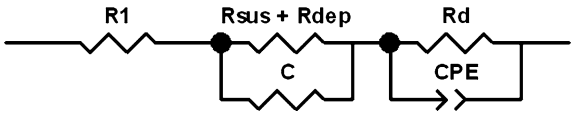

Fig. 7 Equivalent circuit for the analysis of impedance data after the deposition of YSI onto glassy carbon. *R*1: cable resistance, *C*: capacitance, $R_{sus} + R_{dep}$: sum of resistances of suspension and deposit (and possibly some interfacial resistance), R_d, CPE: resistance and constant phase element for the analysis of the low frequency semicircle

observed. The equivalent circuit applied for fitting the spectra is shown in Fig. 7. The high frequency semicircle was described as before (with the resistance now containing contributions from the suspension and the already deposited YSI), and the low frequency semicircle approximated as a parallel combination of a resistor and a constant phase element. The total resistance $R_{sus} + R_{dep}$ increased with increasing deposition time (cf. Fig. 8), and scaled linearly with the charge flown in the experiment and therefore the amount of material deposited on the electrode (Fig. 8, insert). The linear fit had an ordinate intercept of 2.5 kΩ, and a slope of about 1 kΩ/C.

Capacitances values found ranged between 60 and 70 pF. It was not possible to resolve any clear capacitance variation with deposit thickness.

The lower frequency limit of all IS measurements shown above was 1 Hz, in order to avoid long breaks between the individual deposition steps. A control measurement was performed down to 5 mHz after YSi had been deposited (100 V, 5 min), in order to assure that no process contributing to the resistance of the system was overseen. There was no other process taking place at frequencies <1 Hz, and there was no noticeable increase in impedance.

Impedance measurements under open circuit conditions can provide information about resistances of suspension and deposit as well as about the dielectric properties of the suspension. They are less suitable to provide information about dynamic processes during EPD under high applied potentials. In order to check for a voltage influence IS measurements of YSI on GC (150 V, 2 min) at open circuit were compared to others, where a voltage of –4 V was applied to the GC substrate. The value of $R_{sus} + R_{dep}$ increased only slightly. However, the feature at low frequencies became much more prominent. This is shown in Fig. 9. Especially the real part of the impedance at low frequencies (corresponding to the DC limit) is much larger.

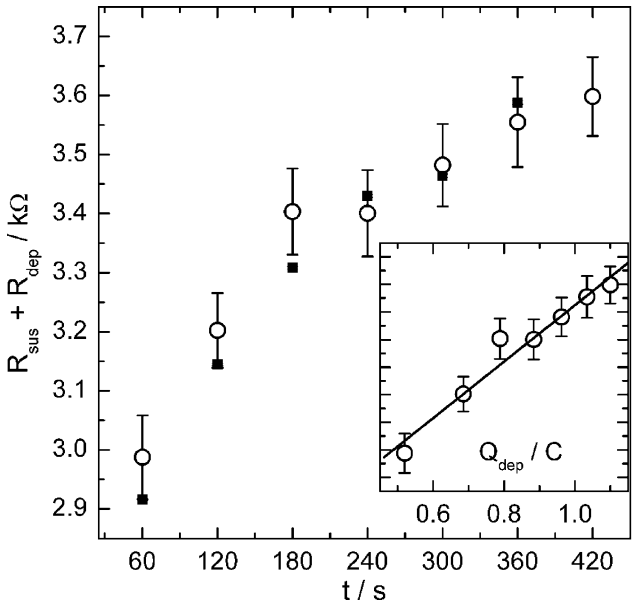

Fig. 8 Dependence of $R_{sus}+ R_{dep}$ from deposition time and thus deposit thickness for two independent deposition series on glassy carbon (100 V, 60 s, 6–7 repeats). The correlation between resistance and total charge flown during deposition is given in the insert (*y*-axis labels identical to large graph)

Electrophoretic deposition of YSi: optimization of deposition conditions

Electrophoretic deposition was performed onto metallic substrates (dimensions: $10 \times 10 \times 1$ mm^3) and on C/C–Si–SiC composite substrates. The industrial material to be protected is a SiC coated carbon-reinforced carbon composite (C/C) (Schunk Kohlenstofftechnik GmbH, Heuchelheim, Germany) in the form of thin slabs with average dimensions $20 \times 20 \times 2$ mm^3.

The preliminary experiments on the metallic substrates were performed as described earlier in order to optimize the conditions of deposition regarding the deposition rate and the quality of the deposited layers [3]. The results of this optimization procedure are shown in Fig. 10.

The best deposition conditions for all systems (dispersion of Y_2SiO_5 and $Y_2Si_2O_7$ in isopropanol and dispersion of the yttrium silicate mixture

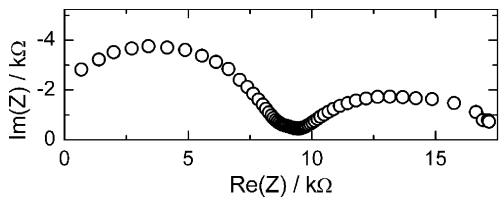

Fig. 9 Impedance spectrum of an YSI-coated GC substrate (150 V, 2 min, 1 cm) at an applied voltage of –4 V (with respect to Au counter electrodes). Frequency range: 1 MHz–0.1 Hz

composed of 70 wt% $Y_2Si_2O_7$ and 30 wt% Y_2SiO_5 [19]) were found to be 60 V/1–3 min. At these conditions we were able to obtain coatings with an average thickness of 5 μm per deposition step at 60 V/1 min. Multiple depositions were also possible.

Discussion

Validation of impedance characterization of EPD suspensions

The YSI powders prepared by the modified Pechini method turned out to be suitable for the preparation of suspensions, which allowed the electrophoretic deposition of YSI material onto a variety of metallic and C-based substrates. Impedance spectroscopy was found to be a useful tool to characterize these suspensions, especially with respect to their conductivity and dielectric behavior.

Most spectra were dominated by a single semicircle. It has been claimed in literature for impedance measurements in YSZ suspensions, that the semicircle was caused by an electrode reaction due to the occurrence of a single semicircle starting from 0 Ω [17]. This was different for the systems studied in this paper. In the case of the isopropanol solvent, the low frequency intercept scaled linearly with the distance between the electrodes (Fig. 1). This is a clear indication that the (high) resistance of the pure solvent contributes significantly to the impedance measured, because an interfacial resistance should be independent of the electrode distance. However, the large intercept observed indicated the presence of another resistance connected in series to the solvent resistance.

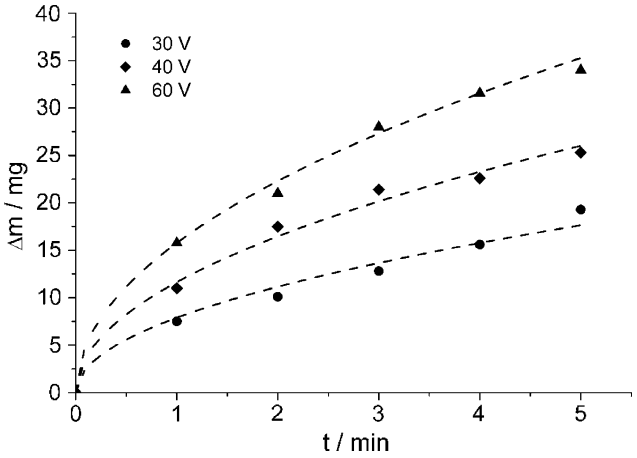

Fig. 10 Deposited mass as a function of deposition time and deposition voltage for yttrium silicate suspension in isopropanol

In addition the semicircle could not well be described with a single time constant (i.e. a simple parallel combination of one resistor and one capacitor), not even when using a CPE instead of a capacitance. Therefore we concluded that an additional interfacial resistance contributes, and fitted the data with the equivalent circuit shown in Fig. 2. The specific conductivity (10^{-7} S cm^{-1}) found is reasonable, and compares to the literature value of 6×10^{-8} S cm^{-1} [20]. The dielectric constant (25.6 ± 3.7) is close to the value given in the literature (20.18 [21]), demonstrating accuracy of measurement and interpretation. Both conductivity and dielectric constant of a polar solvent can vary a little depending on its water content.

For the YSI suspension spectra (Fig. 3) also a small interfacial contribution to the total resistance was found. The relatively low suspension resistance—compared to the solvent—is understandable because of the addition of the powder and the iodine introducing charge carriers. The resistance is still two orders of magnitude higher than that of typical aqueous electrolyte solutions ($c \sim 0.1$ M), only one order of magnitude less than that of distilled water [22], and large enough for EPD. Normalized to the particle concentration one obtains 10^{-2} S cm^2 g^{-1}. The calculation of the particle mobilities is not directly possible from these data. The addition of the charge carriers might also explain the somewhat larger dielectric constant as compared to the pure solvent. However, more studies are necessary to check that point.

Factors controlling the kinetics of electrophoretic deposition

Figures 4 and 5 show the commonly observed decline in deposition rate during electrophoretic deposition. The charge data in Fig. 5 qualitatively match literature data of the time dependence of deposit weight during constant voltage EPD [9]. The combination of electrophoretic deposition and impedance spectroscopy used in this work permits now to decide which of the possible influence factors discussed in literature are responsible for this behavior in the case of the YSI suspensions.

In [14] an experiment was shown, where the current observed after simply changing the polarity was again large, indicating that suspension depletion was not responsible for the current decay. In the studies presented here, the amount of material used up was much less than the powder dispersed in solution. For the experiment shown in the inserts of Figs. 4 and 5, the deposited mass corresponds to at best 4% of the total mass present in solution. If mass depletion was

the sole cause of the current drop, only a slight decrease in current to 96% of its original value should be expected. The current however does decrease to about 4% of its original value. In addition, after pausing the experiment for a couple of minutes (Fig. 4), the current increased again compared to the end of the previous deposition step, which cannot be explained by a simple depletion mechanism. A local depletion in front of the deposition electrode should be minimized by the stirring process. Therefore depletion of the suspension does not play an important role in the experiments studied here.

Often the ohmic resistance of the deposit formed is held responsible for the current drop [9, 11, 14]. An additional ohmic resistance will cause an additional voltage drop and therefore reduce the electric field strength in the suspension, slowing down the deposition rate. Figure 4 clearly demonstrates that the resistance of the entire system deposit/suspension indeed increases with the amount of YSI deposited. Based on the fit line in the insert of Fig. 8 (which allows to calculate the resistance without any deposit and therefore to calculate the relative increase in total resistance due to the deposit and the expected relative decrease of current) one can estimate that the current should decrease to about 70% of its original value if it was controlled by the resistance alone. This indicates that the ohmic resistance cannot be the sole cause of the current decay. Figure 11 shows how large the resistance of the deposit (+suspension) had to be if it alone was responsible for the current decay during the stepwise EPD of YSI, and compares it to the actual data obtained from IS measurements. The discrepancy is evident. In addition the resistances would have to decrease again significantly after turning off the voltage, which is unreasonable. The strong current decay therefore is not caused by EPD layer resistance, either. Interestingly, already before any deposition has occurred the current is less than the maximum current expected from IS, which may be caused by overpotentials at the electrodes under polarization or by inhomogeneities in the electric field. It has been reported by Sarkar and Nicholson that the electric field in front of the electrodes is sometimes larger than in the bulk of the suspension [9].

This leaves mass transport of an electroactive species through the deposit as explanation for the current decay. Even though the formation of the actual deposit in EPD is a nonfaradaic process, the current flowing through the suspension must be equaled by a current passing through the substrate. This requires an electrochemical reaction to take place at the interface. Electroactive species (e.g. protons or iodine) must be

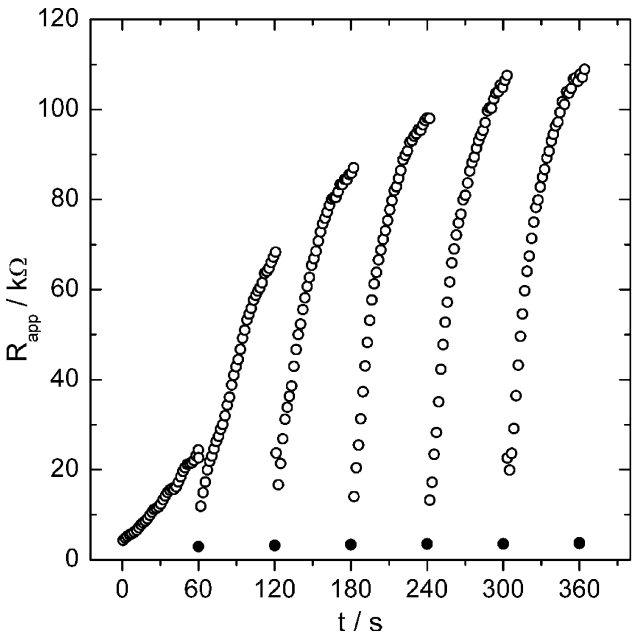

Fig. 11 Resistances (open circles, calculated as $R = U/I$) for $R_{sus} + R_{dep}$ required if the resistance of the deposit layer was solely responsible for the current decay during stepwise YSI deposition onto glassy carbon (100 V, 60 s, 6 repeats). Filled circles: Actual resistances from impedance measurements

transported through the growing deposit to the surface of the substrate, and possible reaction products out of the deposit. If transport through a growing deposit layer controls the current, and is modelled as a diffusion process, after a while the current should decay with $t^{-0.5}$, as in the Cottrell equation [16], which has been derived for different boundary conditions. The charge should be proportional to $t^{0.5}$. Under stationary conditions for mass transport (but not for the current), the concentration at the deposit's surface should be determined by the suspension concentration of the electroactive species, and—given the high voltages and thus the presumably large overpotentials at the electrodes—the concentration close to the substrate/deposit interface should be very low. Therefore a concentration gradient exists across the deposit, which becomes less steep with increasing thickness, causing the current to decrease.

Figure 12 shows some of the Q–$t^{0.5}$ curves during one of the stepwise YSI deposition experiments (deposition steps 2–6), showing good linear behavior. The plots for the current versus $t^{-0.5}$ (Fig. 13) are not as unanimous: a linear behavior is not seen from the beginning of the deposition, and the time until linearity is observed can vary somewhat. Nevertheless the plots support an influence of mass transport control through the deposit. How can the increase in current after an

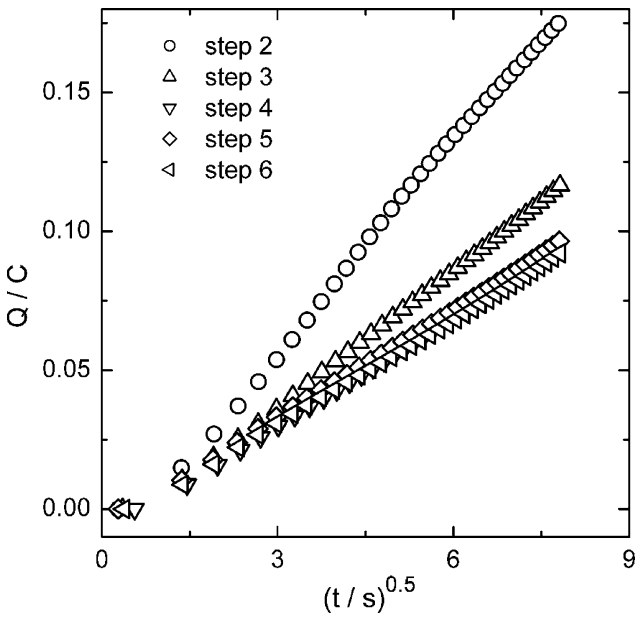

Fig. 12 Charge flux in the individual deposition steps 2–6 during stepwise YSI deposition onto glassy carbon (100 V, 60 s) in function of the square root of time measured from the beginning of the respective step

interruption of the deposition process be explained? Once deposition stops, diffusion of electroactive species from the surface of the deposit towards the substrate will continue as long as a concentration gradient remains. In the next deposition step the concentration at the interface thus will be larger first, and so will the currents. After a while, the gradient restablishes, and currents are low again. This explains why, looking closely at Fig. 4, all the current at later times in each deposition step roughly lie on one master curve. The on-going diffusion processes in the deposit after turning off the voltage, which should increase the conductivity of the deposit, may also be responsible for the differences between the first and second impedance spectra recorded after the end of a deposition step.

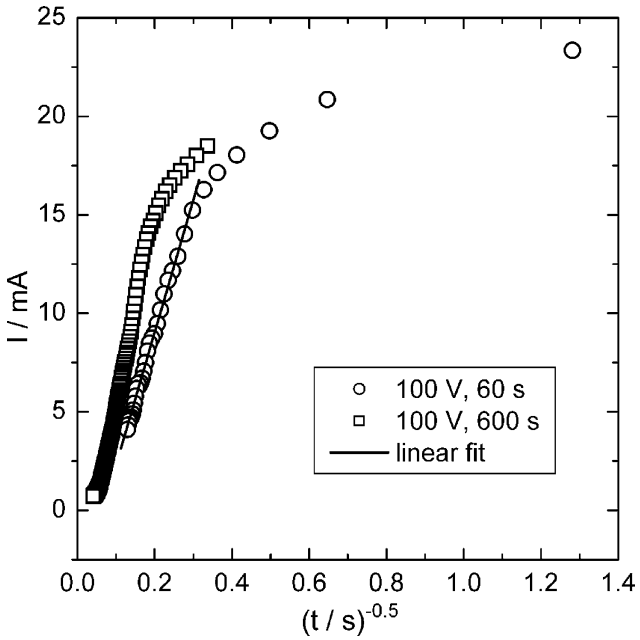

Fig. 13 Current transients recorded during YSI EPD on GC plotted against $t^{-0.5}$ for 100 V, 60 s and 100 V, 600 s

The presence of the low frequency feature in the impedance spectra also points to mass transport, even though some low frequency feature was observed without deposit. We attempted therefore to fit the low frequency feature for the IS measurements with YSI deposit present on the electrodes using two different approaches: using a combination of a resistor and a constant phase element as in Fig. 7, or using a finite-length Warburg impedance [17]. The latter is given by the equation:

$$Z = R \cdot \frac{\tanh([j\omega Y]^{\alpha})}{[j\omega Y]^{\alpha}} \quad (1)$$

with

$$Y = \frac{L^2}{D} \quad (2)$$

where L is the deposit thickness, D the diffusion coefficient, and R the diameter of the corresponding semicircle.

Both approaches did not give good fits. The capacitance values found by the CPE approach increased with increasing thickness, ruling out the low frequency semicircle to be due to the dielectric and resistive properties of the deposit. For the diffusion approach, the α values were close to 0.4, which is reasonable for a diffusion process. The Y values increased with increasing deposition time. According to Eq. 2, a plot of Y versus the square of the deposition charge should give a straight line. This plot is shown in Fig. 14, and shows at least in the beginning a straight line. Given the uncertainty of the analysis, a diffusion coefficient was not calculated from these data.

The much larger low frequency semicircle found under an applied polarisation of –4 V (Fig. 9) also points to the fact, that the process responsible for the appearance of this semicircle is the one causing the current decrease during constant voltage EPD.

The IS studies presented here therefore indicate that the kinetics of YSI deposition are mainly controlled by mass transport through the growing deposit, somewhat by the deposit resistance being larger than

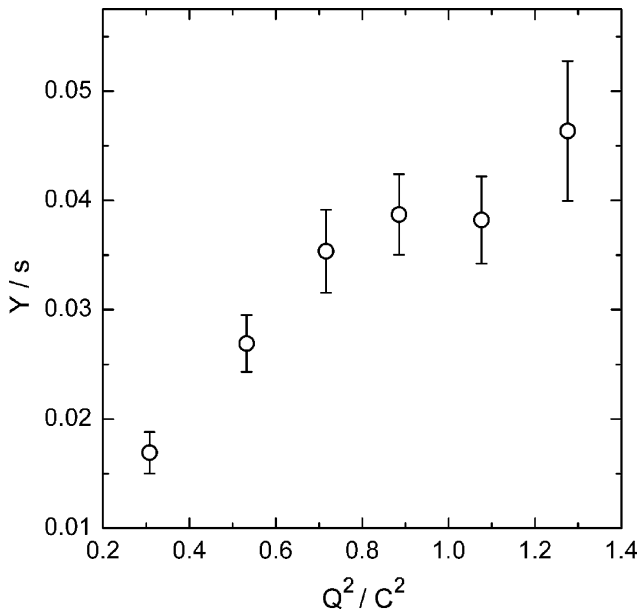

Fig. 14 Dependence of the fitting parameter Y (Eq. 1) for the low frequency feature in the impedance spectra from the total charge measured during EPD of YSI

the suspension resistance, and only very little by suspension depletion.

Conclusions

Suspensions of YSI powders prepared by the Pechini method were suitable for the electrophoretic deposition of YSI on a variety of different substrates. Impedance spectroscopy allowed to measure the dielectric constant and conductivity of the solvent and of the suspensions used for EPD. Current transients during constant voltage EPD showed the typical strong decrease in current with time. By measuring the current transients and the impedance of the system with increasing amount of material deposited, it was possible to rule out the depletion of the suspension and the increasing resistance of the deposit as the major cause for the current decay. The IS measurements point to the control of the deposition by mass transport of electroactive species through the growing deposit.

References

1. Jian-Feng H, He-Jun L, Xie-Rong Z, Ke-Zhi L, Xin-Bo X, Min H, Xiu-Lian Z, Ying-Lou L (2004) Carbon 42:2329
2. Damjanović T, Leipner H, Argirusis Chr, Herbig R, Weiß R, Tomandl G, Borchardt G (2004) Mater Sci Forum 453–454:343
3. Damjanović T, Argirusis Chr, Borchardt G, Leipner H, Herbig R, Tomandl G, Weiss R (2005) J Eur Ceram Soc 25:577
4. Damjanović T, Argirusis Chr, Borchardt G (2005) Mater Sci Forum 494:457
5. Argirusis Chr, Damjanović T, Stojanović M, Borchardt G (2005) Mater Sci Forum 494:451
6. Damjanović T, Argirusis Chr, Jokanović B, Borchardt G, Moritz K, Müller E, Herbig R, Weiss R (2005) Key Eng Mater 314:201
7. Argirusis Chr, Damjanović T, Borchardt G (2004) Mater Sci Forum 453–454:335
8. Argirusis Chr, Damjanović T, Borchardt G (2005) Key Eng Mater 314:101
9. Sarkar P, Nicholson PS (1996) J Am Ceram Soc 79:1987
10. Zhang Z, Huang Y, Jiang Z (1994) J Am Ceram Soc 77:1946
11. Put S, Vleugels J, Van Der Biest O (2003) Acta Mater 51:6303
12. Koura N, Tsukamoto T, Shoji H, Hotta T (1995) J Appl Phys 34:1643
13. Boyer D, Derby B (2003) J Am Ceram Soc 86:1595
14. Fukada Y, Nagarajan N, Mekky W, Bao Y, Kim H-S, Nicholson PS (2004) J Mater Sci 39:787
15. Boccaccini AR, Karapappas P, Marijuan JM, Kaya C (2004) J Mater Sci 39:851
16. Bard AJ, Faulkner LR (2001) Electrochemical methods: fundamentals and applications. 2nd edn. John Wiley & Sons, New York
17. Macdonald JR (1987) Impedance spectroscopy - emphasizing solid materials and systems. John Wiley & Sons, New York
18. Negishi H, Yamaji K, Imura T, Kitamoto D, Ikegami T, Yanagishita H (2005) J Electrochem Soc 152:J16
19. Aparicio M, Duran A (2000) J Am Ceram Soc 83:1351
20. http://www.hedinger.de as on 20 December 2005
21. CRC Handook of Chemistry and Physics (2002) 83rd edn, edited by D. R. Linde, CRC Press, Boca Raton, London, New York, Washington, pp 6–157
22. Wedler G (1982) Lehrbuch der Physikalischen Chemie. Verlag Chemie, Weinheim